3-D MEASUREMENTS USING CONOSCOPY AND APPLICATION TO OPHTHALMOLOGY

Christophe Moser, George Barbastathis, and Demetri Psaltis
Dept. of Electrical Engineering, California Institute of Technology,
Pasadena, California 91125, U.S.A
Tel: + 1 626 3953159; fax: + 1 626 5688437
e-mail: {moser,george,psaltis}@sunoptics.caltech.edu

ABSTRACT

In this paper we present a novel method to measure 3-D quasi planar or quasi spherical reflective surfaces with submicron depth accuracy. Two implementations are presented: a scanning and a non-scanning system. The non-scanning device allows fast measurements and can be applied for eye-shape measurements. The paper is organized as follows: in the introductory section, we first demonstrate the principle of the conoscopic effect leading to the formation of the interferogram. The second and third sections explain respectively, the scanning and non-scanning methods based on the conoscopic effect. We present the experimental results from a simple measurement and show how they conform with theory.

1 PRINCIPLE

Conoscopic holograms, proposed by Sirat and Psaltis [1, 2, 3, 4], are formed by the interference of ordinary and extraordinary waves in bi-refrigent crystals. In fig. 1, a calcite crystal known for its high bi-refringence is placed in-between 2 crossed polarizers. A spherical wave emanating from a point source illuminates the crystal. The rays coming at an angle on the crystal facet experience double refraction, and are therefore split into two components (ordinary and extraordinary) propagating at different velocities. The analyzer at the exit of the crystal mixes the two components and produces a ring-like interference pattern after the analyzer. The spacing between the concentric rings is related to the distance between the point source and the entrance facet of the crystal (see eqn. 1), therefore giving depth information.

2 SCANNING SYSTEM

The geometry of the conoscopic scanning system is shown in fig. 2. A lens of focal length f is positioned in front of the test object. The calcite crystal of thickness L is tilted with respect to the lens optical axis by an angle ψ, let us assume that the testing surface is placed at a distance f from the lens; in this case, the interference pattern is uniform producing no fringes. However if the surface is located at a distance $f+\zeta$ from the lens, fringes start forming in the interferogram. An object is measured point-by-point by scanning the surface in the xy plane. The accuracy in the transverse direction is determined by the accuracy of the translating system. To measure the depth, the ring-like interference pattern is grabbed with a CCD Camera. The depth is given by

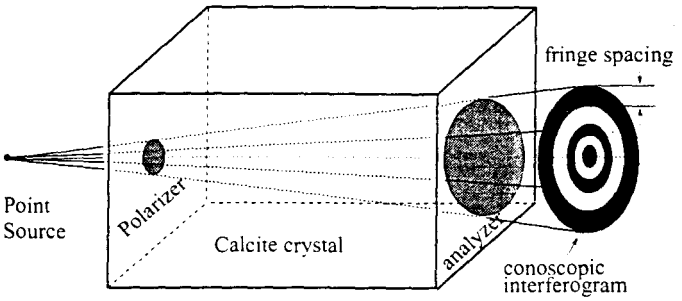

Figure 1: conoscopic holograms

$$\zeta = \frac{\lambda f^2}{2 \Delta x L C(\psi)} \quad (1)$$

where $C(\psi)$ is a function of the crystal tilt angle.
ζ represents the distance from the focal plane of the lens to the object. The total number of fringes N in the image is computed. The fringe separation Δx is obtained by the ratio of N and the aperture of the beam on the camera. The depth resolution is given when the total number of fringes increases by $\frac{1}{2}$. Taking into account the aperture of the lens, the depth resolution becomes:

$$\zeta_{min} = \frac{\lambda f^2}{2 \left(\frac{f}{(f/\#)} - L D(\psi)\right) L C(\psi)}$$

where $D(\psi)$ and $C(\psi)$ are functions of the tilt angle ψ. The depth resolution is a function of the crystal

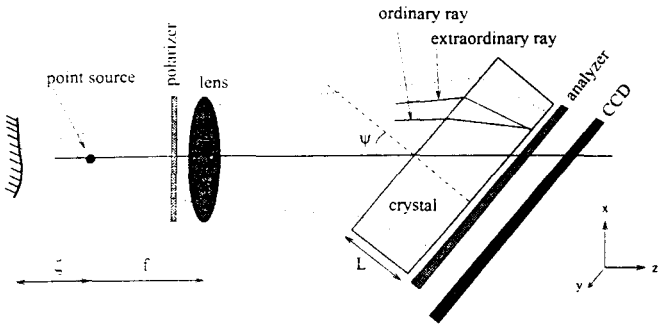

Figure 2: scanning geometry for 3-D measurements

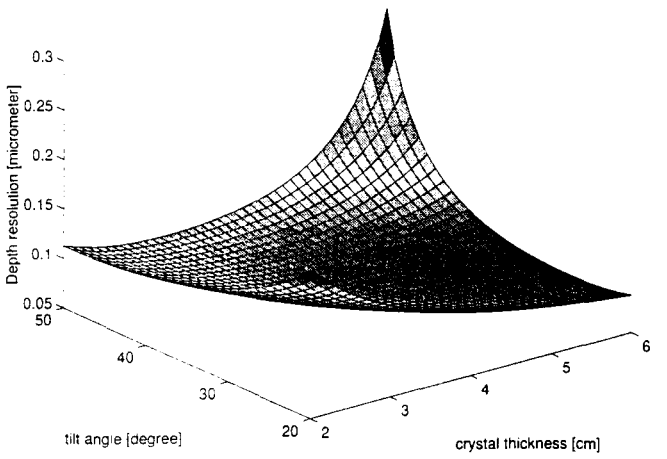

Figure 3: Depth resolution

thickness and the tilt angle as shown in fig. 3. For a vast region, the resolution is on the order of $0.1\mu m$.

A possible implementation of a scanning system would be to constrain the number of fringes on the camera to be constant while the object is scanned. The lens can be accurately moved with a piezo-actuator to keep the number of fringes constant. In this implementation, the depth span is the span of the piezo-actuator. In a second implementation, the lens is kept fixed as the object is scanned. The depth span is then limited by the pixel size, since the further the surface to measure is away from the focal plane, the smaller the fringe separation becomes. The limit is given by $\Delta x > 2b$, where b is the pixel size. Therefore, the span is:

$$\zeta_{max} = \frac{\lambda f^2}{b L C(\psi)}$$

For example, if we choose a crystal thickness of 2.5 cm and a tilt angle of 40 degrees with a focal length f = 1 cm and $f/\# = 1$, the resolution is 0.1 μm and the depth span is 148 μm.

This system can measure smooth reflective surfaces. The piezo-actuator implementation appears to be a good solution, because the spot size on the surface is kept constant and its size can be controlled. This point-by-point measuring system makes it relatively low speed. The following system does not need a scanning mechanism and has approximately the same resolution.

3 SHEAR CONOSCOPY

The concept of conoscopic shear interferometry is shown in Fig. 4. The target reflective surface is assumed to be quasi-spherical (e.g. eye-ball). In the case of a plane wave incident on the tilted crystal, the phase delay experienced by the ordinary and extra-ordinary components are equal across the optical aperture, hence the pattern beyond the analyzer is uniform [1]. However let us assume that the plane wave contains aberrations represented by $\phi(x, y)$. In this case, the intensity pattern is amplitude-modulated by the phase aberration, creating a sheared interferogram. The intensity pattern is given by:

$$\begin{aligned} I(x) &= I_b\,(1 + \gamma \cos\{w(x, y) + \text{const.}\}) \\ w(x) &= \phi(x + h, y) - \phi(x, y) \end{aligned}$$

where I_b is the mean light intensity and γ is the modulation depth and

$$h \approx \frac{L}{2} \sin(2\psi) \left(\frac{n_o}{n_e \sqrt{n_e^2 - \sin^2 \psi}} - \frac{1}{\sqrt{n_o^2 - \sin^2 \psi}} \right)$$

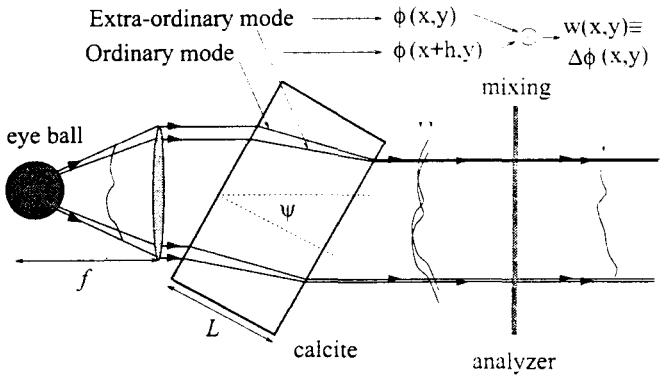

Figure 4: layout for the shear conoscopic system

The steps to extract the profile of the surface are the following: (1) obtain the digitized interferogram, (2) extract the phase $w(x, y)$ of the interference pattern, (3) remove the shear to obtain the target surface shape $\phi(x, y)$.

3.1 PHASE EXTRACTION

Phase extraction is more complicated than a simple inversion of the cosine in eq. 1, because of

[1] Instead of a reflecting sphere and a lens, one would have the same result having a planar surface without a collimating lens

possible non-uniformities in $I_b(x,y)$ and unknown γ. We propose the use of the following phase-shifting method [6]: five intensity measurements $I_{\Delta\omega=0}(x,y), I_{\pi/2}(x,y), I_{\pi}(x,y), I_{3\pi/2}(x,y), I_{2\pi}(x,y)$ of the same interference pattern are obtained by tilting the crystal by

$$\Delta\psi \approx \frac{n_o n_e^2}{n_o^2 - n_e^2} \frac{\lambda}{4L\psi}$$

between measurements, where ψ is the initial tilt angle ($\psi \ll 1$). The phase difference $w(x,y)$ is obtained from

$$w(x,y) = \arctan\left(\frac{2\left(I_{\pi/2}(x,y) - I_{3\pi/2}(x,y)\right)}{I_0(x,y) + I_{2\pi}(x,y) - 2I_{\pi}(x,y)}\right)$$

Fig. 5 to 9 show the five phase shifted interferograms and the resulting phase difference $w(x,y)$ is shown in fig. 10.

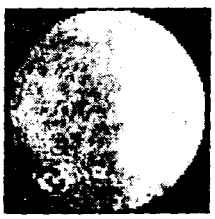

Figure 5: 0

Figure 6: $\frac{\pi}{2}$

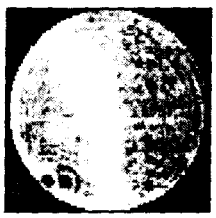

Figure 7: π

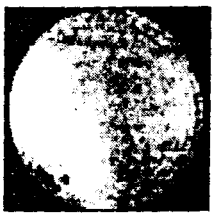

Figure 8: $\frac{3\pi}{2}$

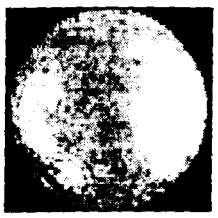

Figure 9: phase shift 2π

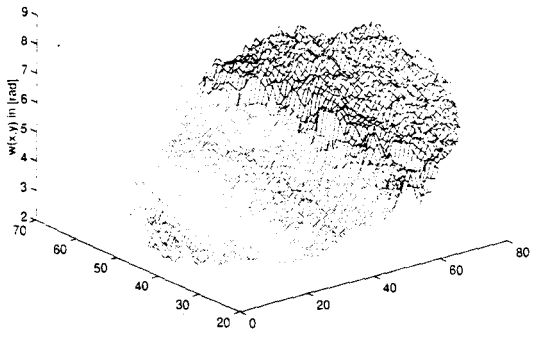

Figure 10: Phase difference $w(x,y)$ recovery

3.2 TARGET SHAPE RECOVERY

The shear removal is performed by decomposing the target $\phi(x,y)$ and the measurement $w(x,y)$ into Hermite polynomial expansion. For simplicity, the method is described for a one dimensional target $\phi(x)$. The decomposition is as follows:

$$\begin{aligned}
\phi(x) &= \sum_{j=1}^{J} b_j H_j(x) \\
w(x) &= \sum_{j=0}^{J} b_j \left[H_j(x+h) - H_j(x)\right] \\
&= \sum_{j=0}^{J-1} c_j H_j(x)
\end{aligned}$$

The order of the polynomial should be taken from some a priori knowledge of the surface. The coefficient $c_j (j = 0, \ldots, J-1)$ are determined directly from the measurement by a least square fit. The coefficients $b_j (j = 1, \ldots, J)$ are computed from the coefficients c_j using a property of the Hermite polynomials:

$$H_j(x+h) - H_j(x) = \sum_{k=0}^{n-1} \binom{n}{k} (2h)^{n-k} H_k(x)$$

The b_j's are then obtained using the recursive formula:

$$\begin{aligned}
b_J &= \frac{c_{J-1}}{2Jh}, \\
b_j &= \frac{1}{2jh}\left[c_{j-1} - \sum_{k=j+1}^{J} \binom{k}{j-1} (2h)^{k-j+1} b_k\right]
\end{aligned}$$

Note that b_0, representing uniform translation along the optical axis, remains undetermined, because the DC information is lost during the shear process.

The shape of an aspherical modeled cornea in PMMA (plastic) using the shear conoscopic method is shown in fig. 11. The measured area on the test surface is $4mm^2$. This area can be increased if a bigger aperture lens is used. This measurement is compared with a measurement done using a Twyman-Green interferometer. Deviation of the order of 0.2 micrometers between the 2 measurements demonstrate the validity of the theory.

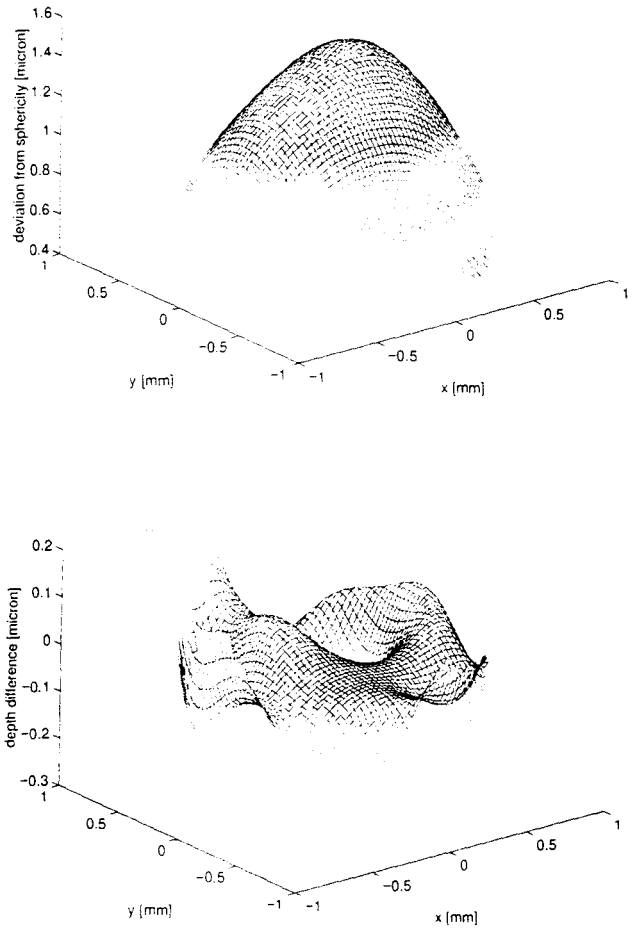

Figure 11: (up) 3-D extraction of an aspherical surface using the shear conoscopic system. The display shows the deviation from sphericity. The bottom picture shows the difference of the above measurements and a reference measurement using a Twyman-Green interferometer.

References

[1] G. Sirat and D. Psaltis, "Conoscopic holography", *Opt. Lett.*, 10(1):4–6, 1985.

[2] G. Sirat and D. Psaltis, "Conoscopic holograms", *Opt. Commun.*, 65(4):243–249, 1988.

[3] G. Sirat, "Conoscopic holography. I. Basic principles and physical basis", *J. Opt. Soc. Am. A*, 9(1):70–83. 1992.

[4] G. Sirat, "Conoscopic holography. II. Rigorous derivation", *J. Opt. Soc. Am. A*, 9(1):84–90, 1992.

[5] D.S Marx, "Subwavelength structures, optical diffraction, and optical disk memories", PHD thesis, California Institute of Technology, 1996.

[6] J. Bryanston-Cross,C. Quan,T.-R. Judge, "Holographic deformation measurements by Fourier transform technique with automatic phase unwrapping" *Opt-Eng*, 31(3):533-543. 1992.